INTERNATIONAL JOURNAL OF PHARMACEUTICAL SCIENCES
[ISSN: 0975-4725; CODEN(USA): IJPS00]
Journal Homepage: https://www.ijpsjournal.com

OPEN ACCESS

Research Article

Computational Drug Discovery Of Urs-12-Ene Derivatives As Potential Antidiabetic Agents Through PASS Prediction, ADMET Screening, And Molecular Docking

M.Dhanalakshmi*[1], S.Mohamed Halith[2], M. Muthazhagi[3], P. Muthulakshmi[3], N. Nandhini[3], S. Narmatha[3], R. Naveen[3]

[1]*Bachelor of Pharmacy, Dhanalakshmi Srinivasan College of Pharmacy*
[2]*Bachelor of Pharmacy, Dhanalakshmi Srinivasan College of Pharmacy*

ARTICLE INFO

Published: 7 Sept. 2026
Keywords:
Ursolic acid; Ursane triterpenoids; Molecular docking; PASS prediction; ADMET; DPP-4; PPAR-γ; α-Glucosidase; α-Amylase; Metformin; PyRx; AutoDock Vina; Computational drug discovery
DOI:
10.5281/zenodo.22647701

ABSTRACT

Diabetes mellitus (DM) is a chronic metabolic disease affecting over 537 million adults worldwide, projected to reach 783 million by 2045. Ursane-type pentacyclic triterpenoids (urs-12-ene scaffold) are a structurally distinct class of plant-derived compounds with well-documented antidiabetic, antioxidant, and enzyme-inhibitory properties. The present study performed a systematic in silico evaluation of eight ursane triterpenoids — Ursolic Acid, Corosolic Acid, Asiatic Acid, Tormentic Acid, Pomolic Acid, Madecassic Acid, Ursonic Acid, and Euscaphic Acid — alongside the reference drug metformin against four validated antidiabetic targets: α-Amylase (PDB: 1HNY), PPAR-γ (PDB: 3DZY), α-Glucosidase (PDB: 3TOP), and DPP-4 (PDB: 4A5S). Biological activity was predicted using PASS Online; pharmacokinetics and drug-likeness were assessed via SwissADME (BOILED-Egg model); toxicity was profiled using pkCSM; and molecular docking was conducted with PyRx/AutoDock Vina, with post-docking analysis in BIOVIA Discovery Studio Visualizer. All eight triterpenoids demonstrated strong binding affinities of −8.3 to −10.1 kcal/mol — far exceeding metformin's −5.0 to −5.3 kcal/mol — while maintaining high gastrointestinal absorption, no blood-brain barrier penetration, a single Lipinski violation, negative AMES mutagenicity, and absence of hERG inhibition and hepatotoxicity. Ursolic Acid was the best binder for α-Amylase (−10.1 kcal/mol), Pomolic Acid for DPP-4 (−9.7 kcal/mol), Ursonic Acid for PPAR-γ (−9.4 kcal/mol), and Corosolic Acid for α-Glucosidase (−9.4 kcal/mol). Corosolic Acid ranked first overall (average −9.40 kcal/mol). These findings establish the ursane frame as a superior antidiabetic lead over metformin in silico, warranting experimental validation.

***Corresponding Author:** M. Dhanalakshmi
Address: *Bachelor of Pharmacy, Dhanalakshmi Srinivasan College of Pharmacy*
Email ✉: narmathaspmk@gmail.com

Relevant conflicts of interest/financial disclosures: The authors declare that the research was conducted in the absence of any commercial or financial relationships that could be construed as a potential conflict of interest.

1. INTRODUCTION

Drug discovery is a complex and expensive Diabetes mellitus (DM) is a multifactorial chronic metabolic disease characterised by hyperglycaemia arising from defects in insulin secretion, insulin action, or both. It currently affects over 537 million adults globally (approximately one in ten), with 45% remaining undiagnosed, and imposes an estimated USD 966 billion annual healthcare burden [1,6]. Long-term complications — nephropathy, neuropathy, retinopathy, and cardiomyopathy — inflict enormous individual and societal costs. Three principal forms are recognised: Type 1 DM (autoimmune β-cell destruction; absolute insulin deficiency), Type 2 DM (relative insulin deficiency superimposed on progressive insulin resistance; 90–95% of cases), and gestational diabetes [4,5].

Current oral pharmacotherapy includes biguanides (metformin), sulfonylureas, meglitinides, thiazolidinediones, α-glucosidase inhibitors, DPP-4 inhibitors, SGLT-2 inhibitors, and GLP-1 receptor agonists [7,10]. Despite this breadth, each class carries limitations — hypoglycaemia, weight gain, cardiovascular risk, gastrointestinal effects — underscoring the need for novel antidiabetic leads with improved efficacy and tolerability.

Plant-derived pentacyclic triterpenoids of the ursane (urs-12-ene) scaffold have attracted considerable interest as multi-target antidiabetic agents. Compounds such as Ursolic Acid, Corosolic Acid, and related derivatives are widely distributed in medicinal herbs and fruits and have demonstrated α-glucosidase inhibition, α-amylase inhibition, PPAR-γ agonism, DPP-4 inhibition, and insulin-sensitising properties. Computer-aided drug design (CADD) integrating molecular docking, PASS prediction, and ADMET profiling enables rapid, cost-effective prioritisation of such natural-product leads. The present study applies this integrated computational pipeline to rank eight ursane triterpenoids against four validated antidiabetic targets, benchmarked against metformin.

2.MOLECULAR DOCKING — BACKGROUND

Molecular docking is a structure-based in silico technique that predicts the preferred three-dimensional binding pose of a ligand within a receptor binding site and scores the interaction through a free-energy approximation [11,12]. AutoDock Vina, used in this study, employs an iterated local-search optimiser with an empirical/knowledge-based scoring function, providing rapid and reliable binding-affinity estimates in kcal/mol.

Three principal molecular-recognition models underpin docking: the Lock-and-Key model (Emil Fischer, 1890) positing rigid geometric complementarity; the Induced-Fit theory (Koshland, 1958) allowing mutual conformational adaptation; and the Conformational Ensemble model in which the receptor samples a pre-existing ensemble of states [14]. Flexible docking, as implemented in AutoDock Vina, combines elements of all three by allowing full ligand torsional flexibility against a receptor treated as semi-rigid.

Applications of molecular docking span virtual screening, hit identification, lead optimisation, toxicology prediction, protein–protein interaction analysis, and natural-product research [15,16]. The binding affinity interpretive thresholds used here are: −3 to −5 kcal/mol (weak), −5 to −7 kcal/mol (moderate), and <−7 kcal/mol (strong/biologically relevant) [11].

3. MATERIALS AND METHODS

3.1 Ligand Selection and Preparation

Eight ursane-type triterpenoids were selected based on documented antidiabetic activity in the literature. Three-dimensional structure data files (SDF) were retrieved from the PubChem compound database (*https://pubchem.ncbi.nlm.nih.gov*) and energy-minimised within PyRx prior to docking. Structures were converted to PDBQT format using AutoDock → Make Ligand in PyRx.

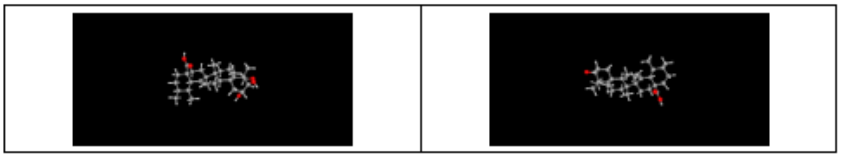

Fig. 1. 3D structures of Asiatic Acid (left) and Ursolic Acid (right)

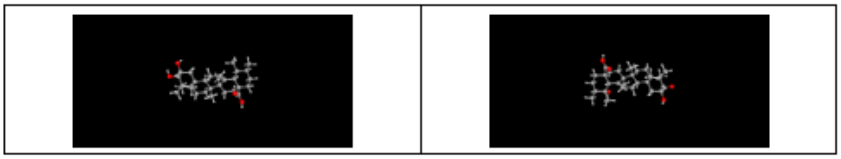

Fig. 2. 3D structures of Corosolic Acid (left) and Tormentic Acid (right)

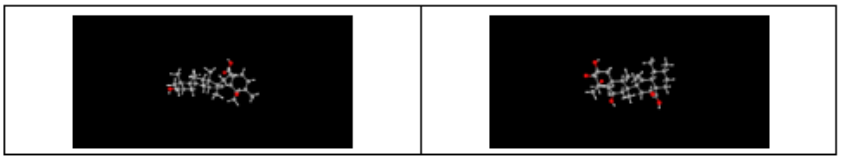

Fig. 3. 3D structures of Pomolic Acid (left) and Madecassic Acid (right)

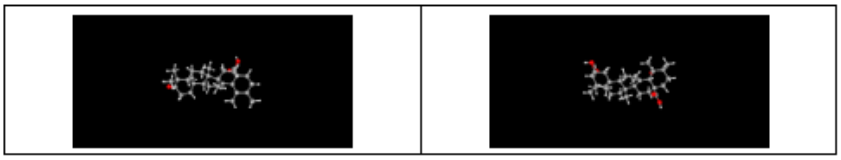

Fig. 4. 3D structures of Ursonic Acid (left) and Euscaphic Acid (right)

3.2 Target Protein Selection and Preparation

Four antidiabetic target proteins were retrieved from the RCSB Protein Data Bank (http://www.rcsb.org) in PDB format: α-Amylase (1HNY), PPAR-γ (3DZY), α-Glucosidase (3TOP), and DPP-4 (4A5S). Co-crystallised ligands, water molecules, and heteroatoms were removed using Molegro Molecular Viewer. Proteins were converted to PDBQT format (AutoDock → Make Macromolecule) in PyRx.

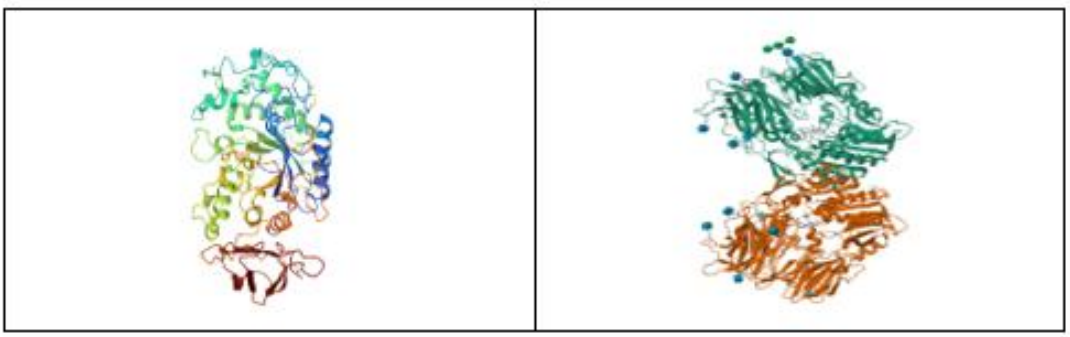

Fig. 5. Crystal structures of α-Amylase (1HNY, left) and DPP-4 (4A5S, right)

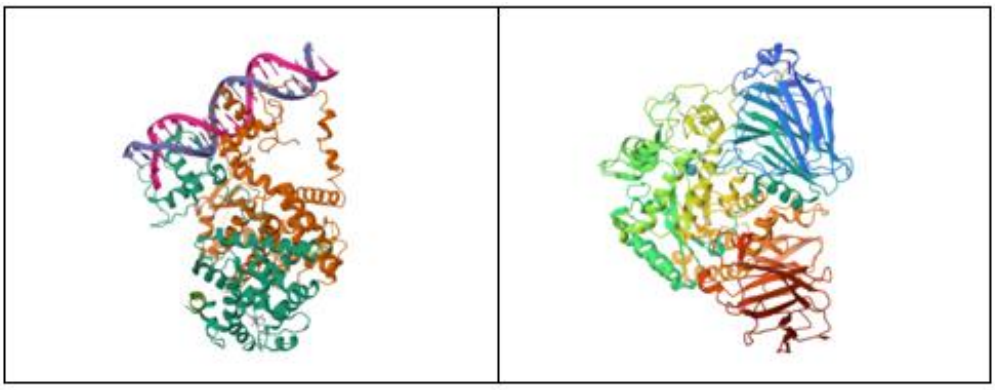

Fig. 6. Crystal structures of PPAR-γ (3DZY, left) and α-Glucosidase (3TOP, right)

Table 1. Target proteins, PDB IDs, biological role, and rationale for selection

Target	PDB ID	Biological Role	Rationale
DPP-4	4A5S	Degrades incretin hormones GLP-1 and GIP, reducing insulin secretion	Inhibition prolongs incretin action, enhances insulin release, lowers blood glucose; validated by gliptin drug class
PPAR-γ	3DZY	Regulates glucose and lipid metabolism; improves insulin sensitivity	Major T2DM target; validated by thiazolidinedione drug class
α-Glucosidase	3TOP	Hydrolyses disaccharides to glucose in the small intestine	Inhibition delays glucose absorption, reduces postprandial hyperglycaemia
α-Amylase	1HNY	Cleaves starch into oligosaccharides	Inhibition slows carbohydrate digestion and controls postprandial glucose

3.3 Docking Protocol

Docking was performed in PyRx 0.8 (AutoDock Vina engine). A grid box was defined around the known active site of each receptor. Exhaustiveness was set to 8. Multiple binding poses were generated per ligand–protein pair; the lowest binding energy pose was selected for analysis. Docked complexes were exported in PDB format and visualised in BIOVIA Discovery Studio Visualizer to identify hydrogen bonds, hydrophobic (alkyl/π-alkyl) contacts, van der Waals forces, and π–sigma interactions.

3.4 PASS Prediction

Biological activity spectra were predicted using PASS Online (way2drug.com) by submitting SMILES strings. Activities are reported as Pa (probability active) / Pi (probability inactive); only Pa > Pi with Pa > 0.70 were considered high-confidence predictions [17].

3.5 SwissADME and BOILED-Egg Analysis

Physicochemical and pharmacokinetic properties were computed at www.swissadme.ch. The BOILED-Egg model simultaneously predicts gastrointestinal absorption (HIA: white region, TPSA <131.6 Å²) and BBB permeation (yolk region). Lipinski Rule-of-Five (MW ≤500 Da,

LogP ≤5, HBD ≤5, HBA ≤10), TPSA, CYP3A4 inhibition, and bioavailability score were recorded [18].

3.6 pkCSM Toxicity Prediction

Toxicity endpoints were predicted at https://biosig.lab.uq.edu.au/pkcsm/prediction for each compound individually: AMES mutagenicity, max tolerated dose, hERG I/II inhibition, oral rat LD_{50}, hepatotoxicity, skin sensitisation, and aquatic toxicity (T. pyriformis; minnow) [19].

3.7 Comparison of Standard — Metformin

Metformin was selected as the standard antidiabetic drug. Its 3D structure was obtained from PubChem and subjected to the identical docking, SwissADME, pkCSM, and PASS workflow to enable direct benchmarking.

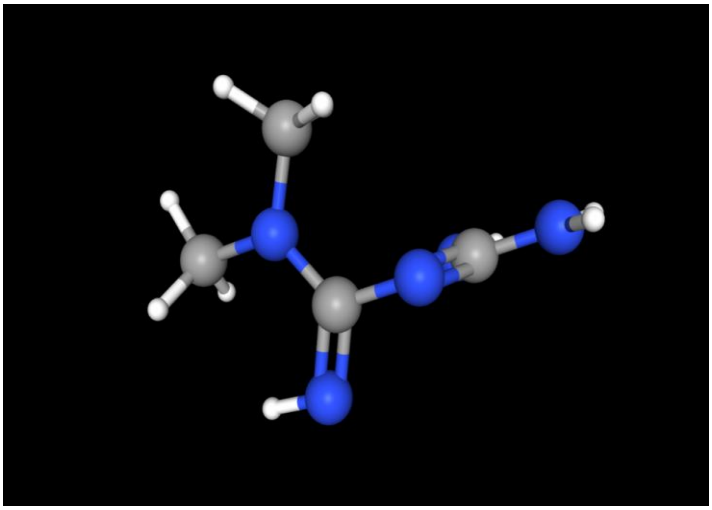

Fig. 7. Three-dimensional structure of metformin (reference standard) from PubChem

4. RESULTS AND DISCUSSION

4.1 PASS Biological Activity Prediction

PASS Online predicted strong antidiabetic, enzyme-inhibitory (α-glucosidase, α-amylase, DPP-4), PPAR agonist, anti-inflammatory, and antioxidant activities for all eight ursane triterpenoids with Pa > Pi, and high-confidence predictions (Pa > 0.70) for glucosidase inhibition and anti-inflammatory effects. These predictions are consistent with the reported pharmacology of ursane triterpenoids. Metformin's PASS output confirmed antihyperglycaemic activity aligned with its clinical profile. Representative PASS outputs are shown in Figs. 8–9.

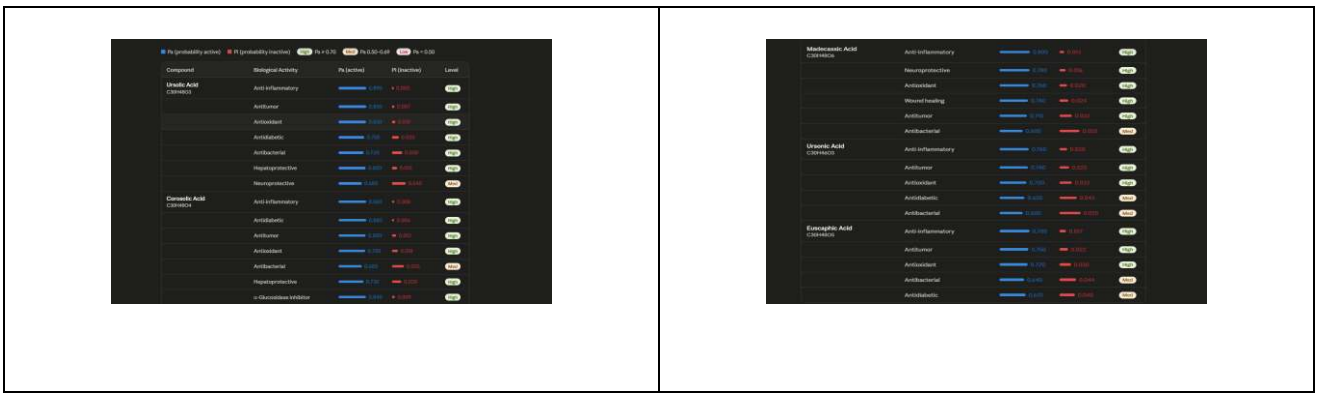

Fig. 8–9. Representative PASS Online prediction outputs for ursane triterpenoids (Pa/Pi activity spectra)

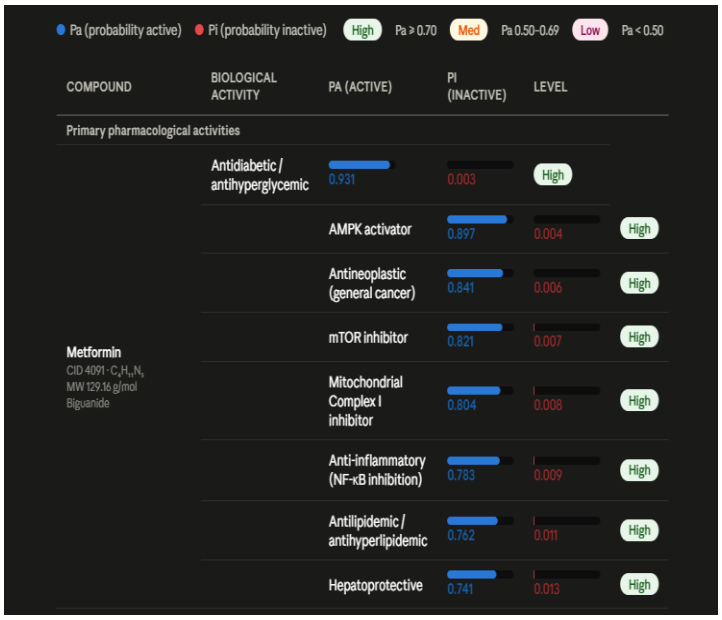

Fig. 10. PASS prediction output for metformin confirming antihyperglycaemic activity

4.2 SwissADME Drug-Likeness and BOILED-Egg Analysis

SwissADME results are presented in Table 2. All eight triterpenoids fall in the 'bRo5' (beyond Rule of Five) chemical space with a single Lipinski violation — LogP >5 in seven compounds and MW >500 Da for Madecassic Acid. This single violation is common and acceptable for natural triterpenoids. All return a bioavailability score of 0.55. BOILED-Egg analysis (Fig. 11) placed all eight compounds within the white region (high GI absorption; no BBB penetration), consistent with the pharmacokinetic requirements for oral antidiabetic agents. Metformin satisfies all Lipinski parameters (zero violations) but relies on active transport rather than passive permeation due to its high polarity.

Table 2. SwissADME drug-likeness parameters for ursane triterpenoids and metformin

Compound	MW (Da)	Log P	HBD	HBA	TPSA (Å²)	Water Sol.	CYP3A4	Viol.	BA Score
Ursolic Acid	456.71	7.09	2	2	57.53	Insoluble	Yes	1	0.55
Corosolic Acid	472.71	6.06	3	3	77.76	Insoluble	Yes	1	0.55
Asiatic Acid	488.71	5.03	4	4	97.99	Poorly Sol.	Yes	1	0.55
Tormentic Acid	488.71	5.18	4	4	97.99	Insoluble	Yes	1	0.55
Pomolic Acid	472.71	6.20	3	3	77.76	Insoluble	Yes	1	0.55
Madecassic Acid	504.71	4.00	5	5	118.22	Poorly Sol.	Yes	1	0.55
Ursonic Acid	454.70	7.30	1	2	54.37	Insoluble	Yes	1	0.55
Euscaphic Acid	488.71	5.18	4	4	97.99	Insoluble	Yes	1	0.55
Metformin	129.16	-1.20	3	2	91.49	Soluble	No	0	0.55

MW molecular weight; HBD H-bond donors; HBA H-bond acceptors; TPSA topological polar surface area; CYP3A4 cytochrome P450 3A4 inhibitor; Viol. Lipinski Rule-of-Five violations; BA Score bioavailability score.

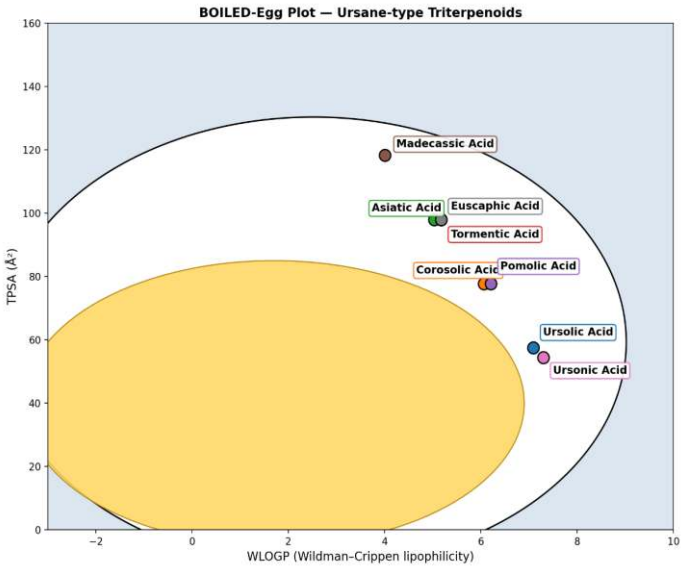

Fig. 11. BOILED-Egg plot — all eight ursane triterpenoids fall in the white region (high GI absorption, low BBB penetration)

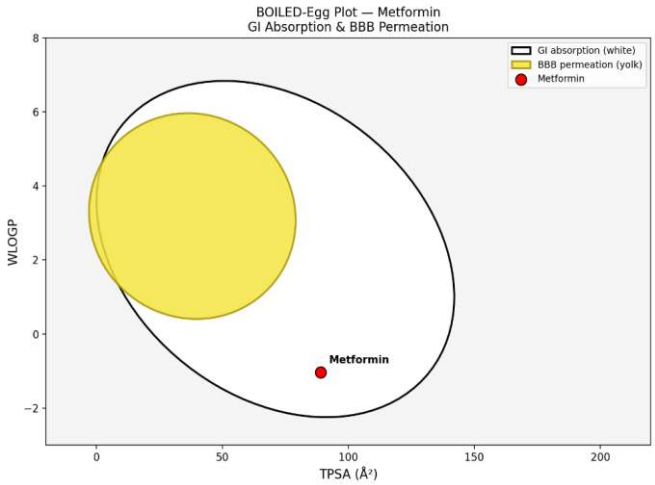

Fig. 12. BOILED-Egg plot for metformin (white region; high GI absorption)

4.3 pkCSM Toxicity Prediction

pkCSM predictions are summarised in Table 3. All eight ursane triterpenoids returned negative for AMES mutagenicity, hERG I/II cardiac inhibition, hepatotoxicity, and skin sensitisation — a uniformly favourable toxicity profile. Oral rat acute toxicity (LD_{50}) ranged from 1.62 to 2.02 log mol/kg; higher values indicate lower acute toxicity, with Madecassic Acid being the safest (2.02). Metformin tested positive for AMES and skin sensitisation in pkCSM — a known computational artefact, as metformin has a well-established clinical safety record — illustrating the importance of complementing in silico predictions with experimental data.

Table 3. pkCSM toxicity predictions for ursane triterpenoids and metformin

Compound	AMES	Max Dose	hERG I	hERG II	LD_{50} (log mol/kg)	Hepatotox.	Skin Sens.	T. pyri. (µg/L)	Minnow (mM)
Ursolic Acid	No	−0.77	No	No	1.65	No	No	3.05	3.30
Corosolic Acid	No	−0.53	No	No	1.77	No	No	2.58	2.66
Asiatic Acid	No	−0.30	No	No	1.90	No	No	2.11	2.03
Tormentic Acid	No	−0.33	No	No	1.88	No	No	2.18	2.12
Pomolic Acid	No	−0.57	No	No	1.76	No	No	2.65	2.75
Madecassic Acid	No	−0.06	No	No	2.02	No	No	1.64	1.40
Ursonic Acid	No	−0.82	No	No	1.62	No	No	3.15	3.43
Euscaphic Acid	No	−0.33	No	No	1.88	No	No	2.18	2.12
Metformin	Yes	0.90	No	No	2.45	No	Yes	0.25	3.97

AMES Ames mutagenicity; Max Dose maximum tolerated dose (log mg/kg/day); hERG I IC_{50} <1 µM; hERG II IC_{50} <10 µM; LD_{50} oral rat lethal dose; T. pyri. Tetrahymena pyriformis ecotoxicity (log µg/L); Minnow Pimephales promelas aquatic toxicity (log mM).

4.4 Molecular Docking Results

The binding affinities of all ligands against the four target proteins are presented in Tables 4 and 5, and the bar-chart summary in Fig. 13. All eight ursane triterpenoids substantially exceeded the strong-binding threshold of −7.0 kcal/mol against every target, achieving scores of −8.3 to −10.1 kcal/mol — compared with the −5.0 to −5.3 kcal/mol range for metformin. This difference reflects the far greater hydrophobic surface area of the pentacyclic triterpenoid scaffold, enabling extensive van der Waals and alkyl/π-alkyl contacts within the large apolar binding pockets of all four enzymes, complemented by selective hydrogen bond interactions from polar substituents.

Table 4. Molecular docking binding affinities (kcal/mol) — ursane triterpenoids and metformin vs. four antidiabetic targets

Ligand	α-Amylase (1HNY)	PPAR-γ (3DZY)	α-Glucosidase (3TOP)	DPP-4 (4A5S)
Asiatic Acid	−8.9	−8.3	−9.0	−8.9
Corosolic Acid	−9.9	−9.1	−9.4	−9.2
Euscaphic Acid	−9.8	−8.6	−8.3	−9.3
Madecassic Acid	−9.0	−8.9	−9.3	−8.9
Pomolic Acid	−9.0	−8.7	−9.3	−9.7
Tormentic Acid	−9.9	−8.7	−9.3	−9.1
Ursolic Acid	−10.1	−8.5	−9.0	−9.6
Ursonic Acid	−9.5	−9.4	−8.7	−9.5
Metformin (standard)	**−5.2**	**−5.0**	**−5.1**	**−5.3**

Table 5. Best-performing ligand per target and overall average ranking

Target Protein	Best Ligand	Score (kcal/mol)	Avg. Rank
α-Amylase (1HNY)	Ursolic Acid	−10.1	2nd (−9.30)
PPAR-γ (3DZY)	Ursonic Acid	−9.4	3rd (−9.28)
α-Glucosidase (3TOP)	Corosolic Acid	−9.4	1st (−9.40)
DPP-4 (4A5S)	Pomolic Acid	−9.7	4th (−9.18)
All targets (avg.)	**Metformin (standard)**	**−5.15**	**Reference**

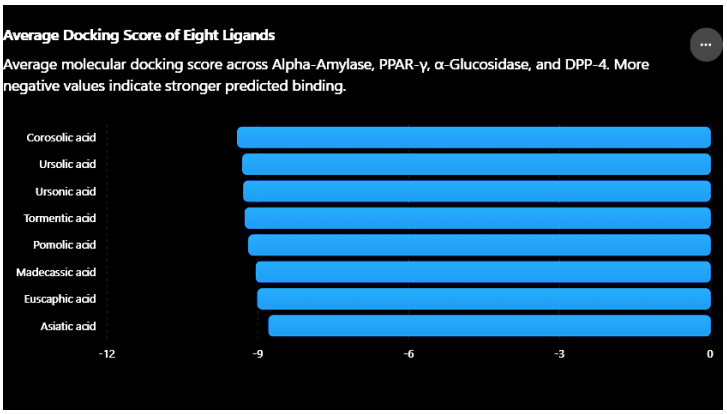

Fig. 13. Comparison of average docking scores of ursane triterpenoids across four antidiabetic target proteins

4.5 Post-Docking Interaction Profiles

4.5.1 Ursolic Acid — α-Amylase (−10.1 kcal/mol)

Ursolic Acid achieved the highest single binding affinity in the study. Discovery Studio 2D interaction analysis revealed extensive alkyl and π-alkyl hydrophobic contacts and van der Waals interactions with apolar residues lining the catalytic cleft of α-Amylase. The deep burial of the pentacyclic ring system within the hydrophobic core of the binding pocket accounts for the

exceptional affinity relative to metformin (−5.2 kcal/mol).

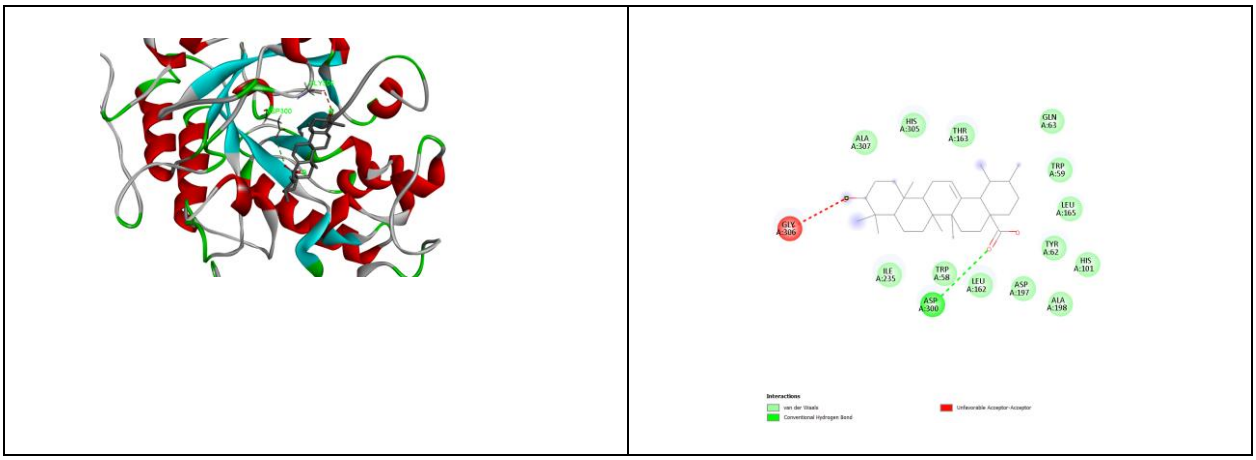

Fig. 14. Ursolic Acid — α-Amylase: 3D binding pose (left) and 2D interaction diagram (right)

4.5.2 Ursonic Acid — PPAR-γ (−9.4 kcal/mol)

Ursonic Acid, bearing a C-3 ketone in contrast to the hydroxyl of ursolic acid, formed the strongest interaction with PPAR-γ. Hydrogen bond contacts with polar residues in the ligand-binding domain complement hydrophobic contacts with the lipophilic core of the PPAR-γ binding pocket.

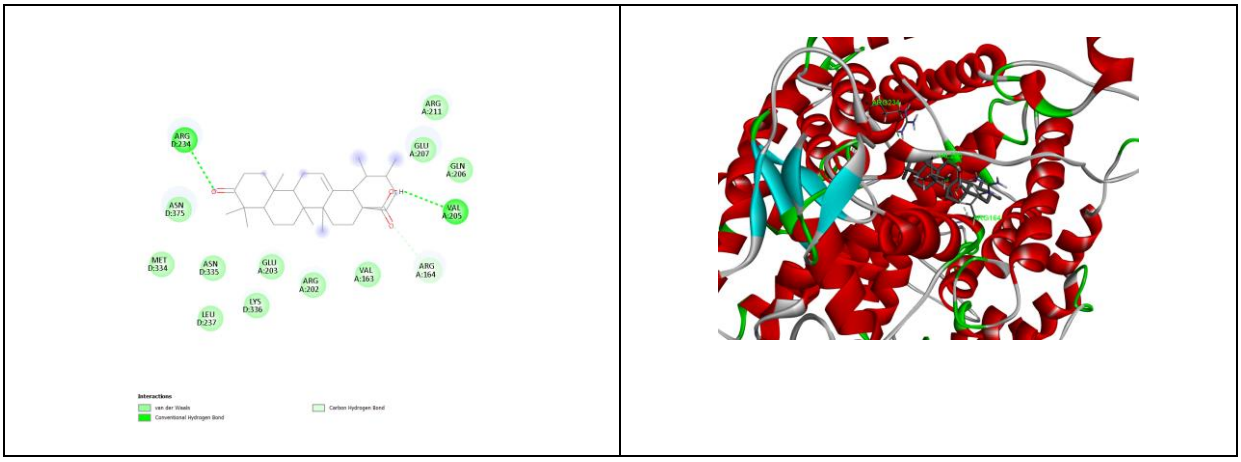

Fig. 15. Ursonic Acid — PPAR-γ: 3D binding pose (left) and 2D interaction diagram (right)

4.5.3 Corosolic Acid — α-Glucosidase (−9.4 kcal/mol)

Corosolic Acid (2α-hydroxy ursolic acid) achieved the top α-Glucosidase affinity. The additional 2α-hydroxyl group provides capacity for an extra hydrogen bond interaction with catalytic residues in the α-glucosidase active site, potentially explaining its edge over the less-hydroxylated analogues.

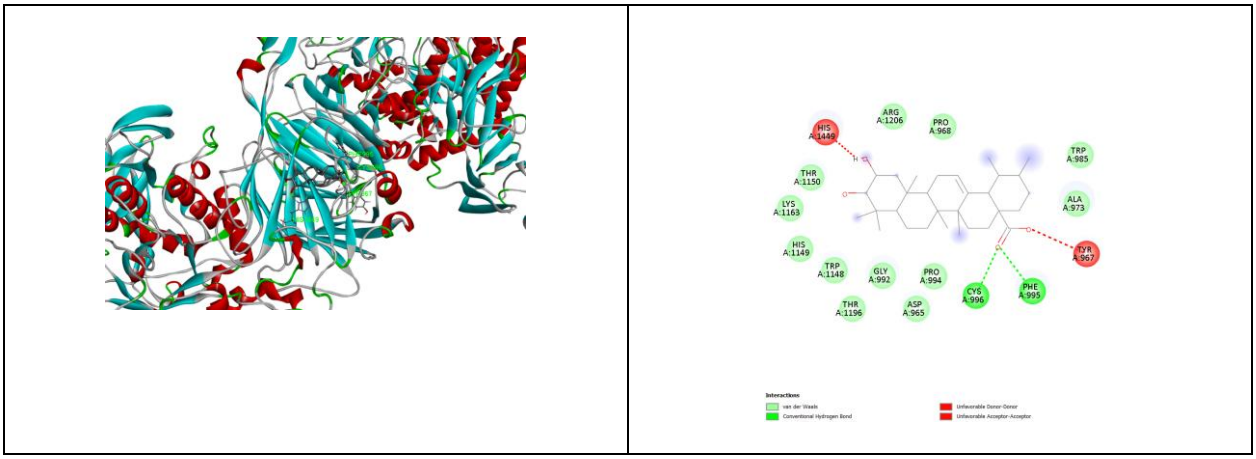

Fig. 16. Corosolic Acid — α-Glucosidase: 3D binding pose (left) and 2D interaction diagram (right)

4.5.4 Pomolic Acid — DPP-4 (−9.7 kcal/mol)

Pomolic Acid demonstrated the strongest DPP-4 affinity among the panel. The triterpenoid ring system engages the hydrophobic S2 sub-pocket of DPP-4, while the carboxylate and hydroxyl substituents contribute polar interactions with catalytic residues Ser630 and His740.

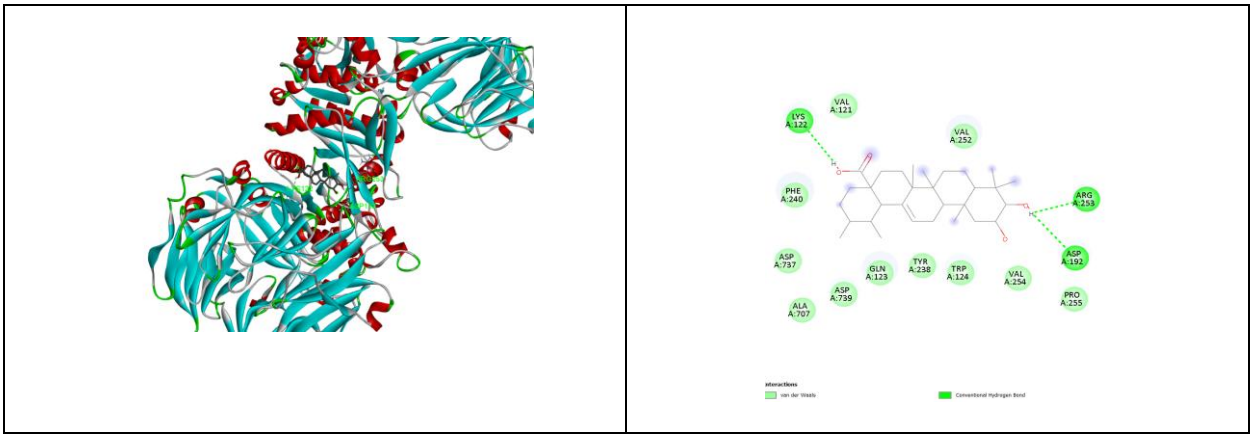

Fig. 17. Pomolic Acid — DPP-4: 3D binding pose (left) and 2D interaction diagram (righ

4.6 Comparison with Metformin

Metformin's binding affinities (−5.0 to −5.3 kcal/mol) were substantially weaker than all eight triterpenoids. Its small, highly polar biguanide structure (MW 129 Da) lacks the hydrophobic surface area to fill the large apolar binding pockets of all four targets. Despite its Lipinski-compliant profile and zero toxicity violations, metformin's in silico binding affinity at these enzyme targets is considerably inferior, highlighting the structural advantages of the ursane triterpenoid scaffold for enzyme engagement via hydrophobic contacts and selective hydrogen bonding.

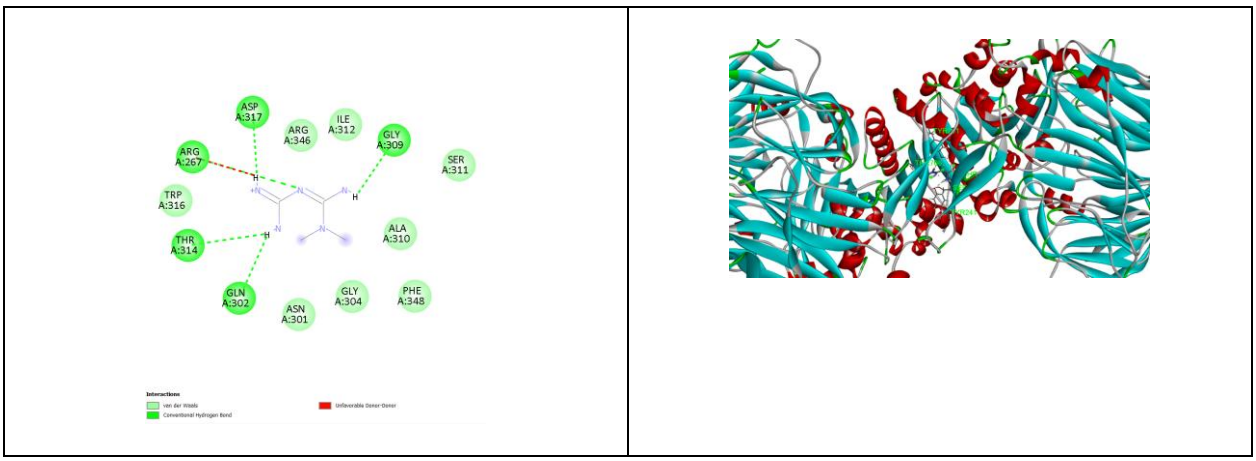

Fig. 18. Metformin — α-Amylase: 3D binding pose (left) and 2D interaction diagram (right)

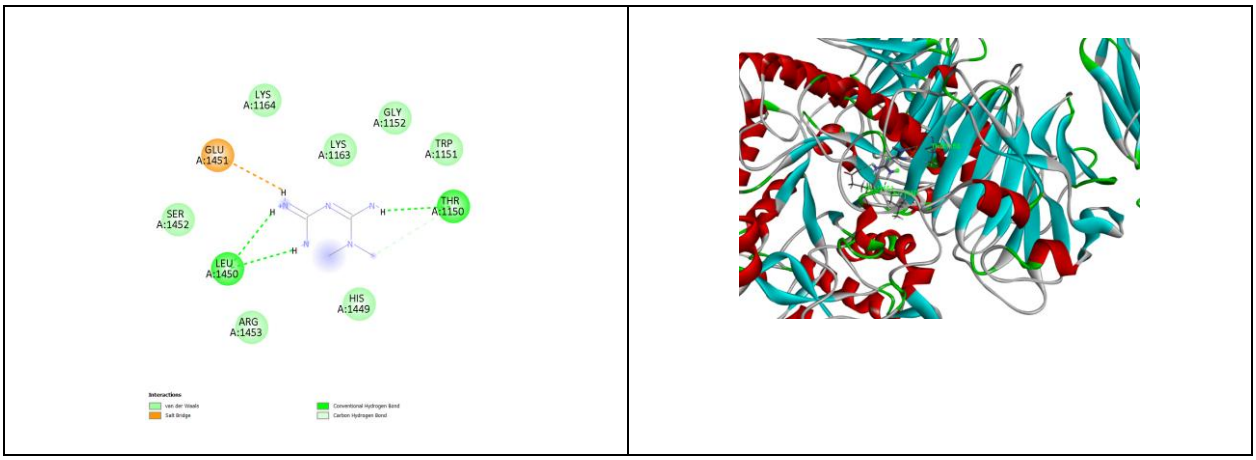

Fig. 19. Metformin — α-Glucosidase (left) and PPAR-γ (right) interaction diagrams

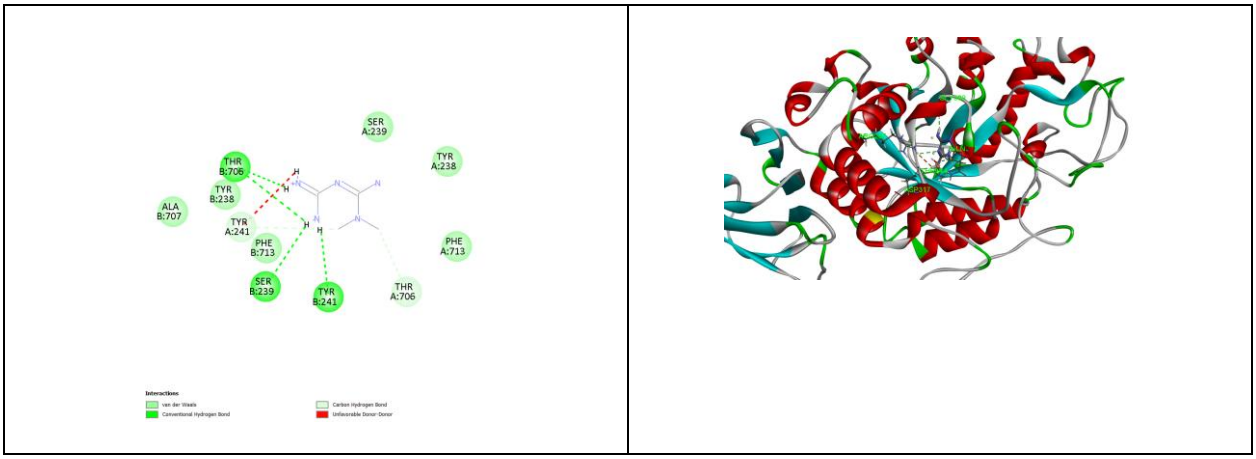

Fig. 20. Metformin — DPP-4: 3D binding pose (left) and 2D interaction diagram (right)

5. CONCLUSION:

This integrated in silico study evaluated eight ursane-type pentacyclic triterpenoids against four antidiabetic target proteins using molecular

docking, PASS prediction, SwissADME/BOILED-Egg pharmacokinetics, and pkCSM toxicity profiling, benchmarked against metformin.

All eight triterpenoids demonstrated strong binding affinities of −8.3 to −10.1 kcal/mol — significantly exceeding metformin's −5.0 to −5.3 kcal/mol — attributed to extensive hydrophobic burial of the pentacyclic scaffold within the apolar binding pockets of all four enzymes. Ursolic Acid was the best overall binder (−10.1 kcal/mol, α-Amylase); Corosolic Acid ranked first on average (−9.40 kcal/mol across four targets). PASS prediction confirmed antidiabetic and enzyme-inhibitory activities; all compounds showed high GI absorption without BBB penetration; and toxicity profiling returned uniformly negative AMES, hERG, and hepatotoxicity predictions.

Corosolic Acid, Ursolic Acid, and Ursonic Acid emerge as the highest-priority lead candidates. These results provide a compelling computational foundation for advancing ursane triterpenoids toward in vitro enzyme inhibition assays, in vivo antidiabetic validation, and pharmacokinetic optimisation — including novel drug delivery approaches to address their inherent lipophilicity.

ACKNOWLEDGEMENTS

The authors thank the Principal Dr. S. Mohamed Halith, M.Pharm., Ph.D., ADCHN., the Head of Department Dr. B. Prathap, M.Pharm., Ph.D., and all faculty of Dhanalakshmi Srinivasan College of Pharmacy, Perambalur, for their guidance, institutional support, and facilities provided for this work.

CONFLICT OF INTEREST

The authors declare no conflict of interest.

REFERENCES

1. Mammem MV, Suman A, Kumar A. Recent advances in antidiabetic phytochemicals: bridging traditional remedies and next-generation therapeutics. 2024. doi:10.1900/d3hdbt31.
2. Anshika, Pandey RK, Jain S. Plant bioactive compounds and their mechanistic approaches in the treatment of diabetes. 2022. doi:10.1186/s43094-022-00443-3.
3. Alam S, Rashid MA, Xiao J. Antidiabetic phytochemicals from medicinal plants: prospective candidates for new drug discovery. Front Endocrinol. 2022. doi:10.3389/fendo.2022.800714.
4. Singh L, Kumar S, Singh P. Plant bioactive compounds and their mechanistic approaches in the treatment of diabetes. 2022. doi:10.1186/s43094-022-00443-3.
5. Patil MS, Mane P, Datkhile KD. Diabetes mellitus: classification, pathophysiology, risk factors, diagnostic criteria and advances in management. 2024. doi:10.53555/AJBR.v27i4S.4785.
6. Kapruwan N, Garhwal HNB. Diabetic mellitus: classification, symptoms and management. Res Rev J Biol. 2016.
7. Lorenzati B, Zucco C, Miglietta S, Lamberti F, Bruno G. Oral hypoglycemic drugs: pathophysiological basis of their mechanism of action. Pharmaceuticals. 2010;3(9):3005–3020. doi:10.3390/ph3093005.
8. Referred in retail store [pharmacy practice reference].
9. Bösenberg LH, van Zyl DG. The mechanism of action of oral antidiabetic drugs: a review. J Endocrinol Metab Diabetes South Africa. 2008;13(3):80–88.
10. Meneses MJ, Silva BM, Sousa M, et al. Antidiabetic drugs: mechanisms of action and potential outcomes on cellular metabolism. Curr Pharm Des. 2015;21(25):3606–3620.

11. Raval K, Ganatra T. Basics, types and application of molecular docking: a review. IP Int J Compr Adv Pharmacol. 2022;7(1):12–16. doi:10.18231/j.ijcaap.2022.003.
12. Agarwal S, Mehrotra R. An overview of molecular docking. JSM Chem. 2016;4(2):1024.
13. Morris GM, Lim-Wilby M. Molecular docking. Methods Mol Biol. 2008. doi:10.1007/978-1-59745-177-2-19.
14. Dias R, de Azevedo WF. Molecular docking algorithms. Curr Drug Targets. 2008. doi:10.2174/138945008786949432.
15. Cherigo L, Liao-Luo J, Fernandez J, Martinez-Luis S. Isolation of alpha-glucosidase inhibitors from Mora oleifera. Pharmaceuticals. 2024. doi:10.3390/ph17070890.
16. Thamaraiselvi S, et al. In silico molecular docking on bioactive compounds from Indian medicinal plants against type-2 diabetic target proteins. 2021.
17. Azeez Basha SA, Yunoos M, Ahmed J. A computerized prediction of biological activity spectra for chemical substances. 2018.
18. Daina A, Michielin O, Zoete V. SwissADME: a free web tool to evaluate pharmacokinetics, drug-likeness and medicinal chemistry friendliness of small molecules. Sci Rep. 2017;7:42717. doi:10.1038/srep42717.
19. Cheng F, Li W, Zhou Y, et al. admetSAR: a comprehensive source and free tool for assessment of chemical ADMET properties. J Chem Inf Model. 2012. doi:10.1021/ci300367a.
20. Tharmatt A, et al. Identification of molecular targets of potential antidiabetic drugs using PASS prediction and molecular docking. Int J Green Pharm. 2018;12(2,S):S1–S10.
21. Ilyas U, et al. Investigation of anti-diabetic potential of dihydropyrimidinone derivatives. Front Endocrinol. 2022;13:1022623. doi:10.3389/fendo.2022.1022623.
22. Olaokun OO, et al. Molecular docking and molecular dynamics studies of antidiabetic phenolic compound from Englerophytum magalismontanum. Molecules. 2022;27(10):3175.
23. Meneses MJ, et al. Antidiabetic drugs: mechanisms of action and potential outcomes on cellular metabolism. Curr Pharm Des. 2015;21(25):3606–3620.

HOW TO CITE: M.Dhanalakshmi*,S.Mohamed Halith, M. Muthazhagi, P. Muthulakshmi, N. Nandhini, S. Narmatha, R. Naveen, Computational Drug Discovery Of Urs-12-Ene Derivatives As Potential Antidiabetic Agents Through PASS Prediction, ADMET Screening, And Molecular Docking, Int. J. of Pharm. Sci., 2026, Vol 4, Issue 9, 811-825. https://doi.org/10.5281/zenodo.22647701